Quantum Well Intermixing of InP-Based AlInGaAs Quantum Wells Using IFVD Technique and the Mask Boundary Effect

Zhengkai Jia[1], Hua Yang[2], Hui Wang[1], Xing Dai[1], Alison H. Perrott[1,2], Frank H. Peters[1,3]
[1] Integrated Photonics Groups, Tyndall National Institute, Cork, Ireland.
[2]Rockley Photonics Ireland, Cork, Ireland
[3] Department of Physics, University College Cork, Cork, Ireland.
e-mail: Zhengkai.jia@tyndall.ie

ABSTRACT

This paper presents research on quantum well intermixing (QWI) using impurity-free vacancy-disordering (IFVD) while studying the effect of the QWI mask boundary. Using a SiN_x film deposited by PECVD as a QWI mask and annealing under 725˚C for 2 minutes, a 120nm wavelength blue shift of a FP laser is achieved using an InP-based AlInGaAs quantum well laser material. It is found that a 7.5µm margin is needed between the QWI mask edges and the non-QWI area during the QWI process. This will be a valuable reference for design and fabrication of photonic integration circuits (PICs) using QWI.

Keywords: Quantum Well Intermixing, IFVD, Mask Boundary Effect, Photonic Integration.

1. INTRODUCTION

Photonic integration is becoming increasingly important in lowering the cost and footprint of data centre photonics [1]. Quantum Well Intermixing (QWI) is a post-growth technique that allows the energy band gap of a quantum well (QW) to be modified without any regrowth and thus can be used in the fabrication of PICs to reduce or eliminate epitaxial regrowth [2]. During the QWI process, the diffusion of different atoms into the QW changes the material composition of the well. The band gap of the QW typically increases (thus blue-shift) as a result of the QWI. Several QWI techniques including impurity induced disordering (IID), photo-absorption-induced disordering (PAID) and impurity-free vacancy-disordering (IFVD) have been reported [3]. Among them impurity-free vacancy-disordering (IFVD) is the simplest method to create different amounts of inter-diffusion in different regions of a sample by using dielectric coatings like SiN_x as a promoter, which is compatible with common semiconductor processing. IFVD results in little or no damage to the surface of the epitaxial wafer and requires no extra treatment to the epitaxial wafer, such as a sacrificial layer.

Here, we present our research on the QWI of an InP-based AlInGaAs-MQW material and demonstrate the effect of QWI's mask boundary on the laser wavelength shift by making and measuring Fabry-Perot (FP) ridge waveguide lasers using our QWI technique. This QWI technique and the boundary effect will be a useful reference for further photonic integration design and fabrication.

2. DESIGN AND EXPERIMENT OF QWI BY IFVD

Firstly, the quantum well intermixing with IFVD method is investigated using InP-based AlInGaAs/AlInGaAs multiple quantum well epitaxial material by MOCVD which includes 5 pairs of compressive strained quantum wells (QW, +1.2% strain, 6nm thick quantum well and 10nm thick barrier, λ_{PL}=1.55µm, by photoluminescence) on n-doped InP substrates, as show in Fig.1. In the experiment, the effect of SiN_x and SiO_2 films are investigated. 200nm thick SiN_x and 200nm thick SiO_2 films are deposited respectively by plasma enhanced chemical vapor deposition (PECVD) and sputtering on the top surface of the as-grown epitaxial wafers. Then the samples with different dielectric coatings were annealed under the same conditions by rapid thermal annealing (RTA) at 675˚C, 700˚C and 725˚C, and the PL of the samples after annealing were measured with the top p-doped InGaAs and InP layers removed. The results are plotted in Fig.2 and Fig.3. From Fig.2, it can be seen that the PL wavelength of the as-grown material is at 1530nm while the PL wavelength of the sample with SiN_x by PECVD blue shifts after annealing and further as the temperature increases. It shifts to 1521nm at 675˚C, to 1457nm using 700˚C and to 1410nm annealing at 725˚C. From Fig.3, the PL wavelength of the samples with a surface coating of SiO_2 by PECVD are shown to blue shift by 5 to 15nm after annealing at 675˚C to 725˚C. The samples with SiO_2 and SiN_x coatings by sputtering showed non-repeatable results with some samples cracking after annealing, thus they are not suitable for the QWI process. Samples without any dielectric coatings had surface damage as a result of the annealing process. Based on the experiment, SiN_x by PECVD results in a PL wavelength shift of more than 100nm during the annealing at 725˚C, while a SiO_2 film by PECVD coating prevents the wavelength shift during the annealing and protects the surface. Thus, the SiN_x by PECVD works as the promotor while the SiO_2 by PECVD acts as inhibitor in our QWI technique.

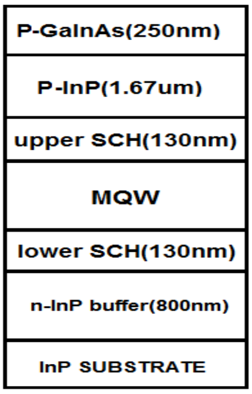

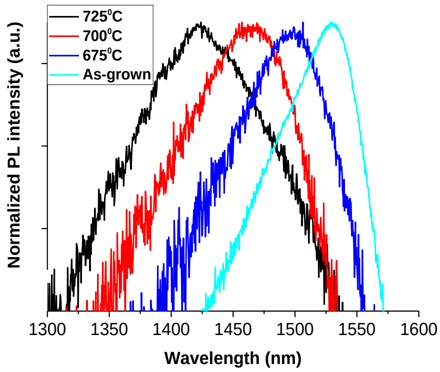

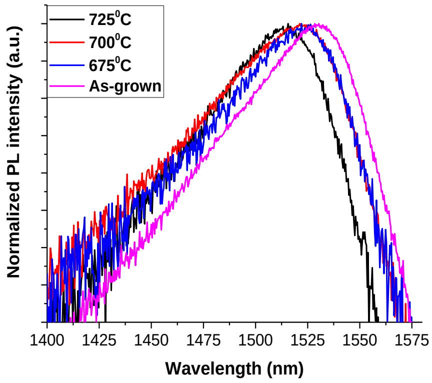

Figure 1. Schematic structure of the epitaxial wafers (left), Figure 2. PL spectra of the samples capped with SiN_x (middle) and Figure 3. SiO_2 films by PECVD and annealed under different temperature (right).

3. STUDY ON THE BOUNDARY EFFECT QWI PROCESS

3.1 Design

Based on the IFVD QWI technique described in section 2, FP lasers with the same structure but with different SiN_x mask boundaries were designed, as shown in Fig.4 where 12 FP lasers are designed with a 40µm wide SiN_x mask but with different distances between the centre of the ridge waveguide of the FP laser to the edge of the mask from: -20µm (negative numbers mean that the ridge is fully covered with the mask) to 21.25µm. All the lasers were 500µm long with 2.5µm wide ridges, using one deep etched facet and one cleaved facet.

3.2 Fabrication

The same epitaxial material as that for QWI experiments in section 2 was used in fabricating the FP lasers. The fabrication process is a typical Fabry-Perot semiconductor laser process using conventional photolithography and etching techniques, except that QWI areas were first defined by using PECVD SiO_2 as protector and PECVD SiN_x as promoter. First, 50nm thick SiN_x was deposited on top of the wafer by sputtering, followed by standard photolithography and a wet etch, which was performed to define the QWI zone (promoted zone). Then 200nm thick SiO_2 was deposited on top of the wafer by PECVD (the IIIV-SiO_2 contacted surface defined the inhibited zone). The wafer was then annealed in a nitrogen ambient at 725˚C for 2 minutes and then the SiO_2 and SiN_x masks were removed from the wafer. Next, 650nm thick SiO_2 was deposited on top of the wafer by sputtering, followed by standard photolithography, which was performed to define the waveguide. Inductively coupled plasma (ICP) dry etching of SiO_2 with CF_4 / CHF_3 was then performed to transfer the pattern into the SiO_2 mask. 1.92µm deep ridge waveguides were then formed using a room temperature ICP dry etch with Cl_2 / CH_4 / H_2. After wafer passivation using 300nm of SiO_2, a window was formed in SiO_2 by ICP dry etching, followed by p metal (TiAu) deposition. Finally, the sample was thinned to 120µm, and a Au / Ge / Au / Ni / Au metal stack was deposited on the back side of the wafer, which was then annealed at 400˚C for 5 minutes in a nitrogen oven.

3.3 Characterization

The fabricated FP lasers were cleaved into bars as shown in Fig.5 with two arrays of 500µm long single facet (the other is etched facet) lasers back to back. The light current- voltage (LIV) characteristics were tested at room temperature (20˚C) with electric probing under CW current injection and using an integrating sphere to collect the light output from the cleaved facet. In the test, all the FP lasers after the QWI process lase continuously with threshold currents from 23 to 40mA. This proves that the fabrication of the lasers was successful. The non-QWI laser (the laser area is fully covered by SiO_2 during QWI process) lases continuously with a threshold current of 23mA and the output power linearly increases with current up to around 31.5mW at 300mA bias. The full-QWI FP laser (with the ridge waveguide in the centre of the SiN_x mask during the QWI process) lases CW at a 40mA threshold current and the output power reaches 16.5mW at 300mA. The turn-on voltage of the full QWI laser increases to 1.1V from 0.9V of the non-QWI FP laser, which indicates y bandgap increase of the material during the QWI process. The LIV results are shown in Fig.6. The threshold current, output power and the turn-on voltage of the half-QWI FP laser (with ridge half covered by the SiN_x mask) are in between.

The lasing spectra of the FP lasers were then measured by coupling light into lensed fibre and using an optical spectrum analyser. Fig.7 shows the spectra at 40mA current injection for the FP lasers, which were annealed at 725˚C with different QWI mask conditions (with different distance between the ridge centre and the edge of the

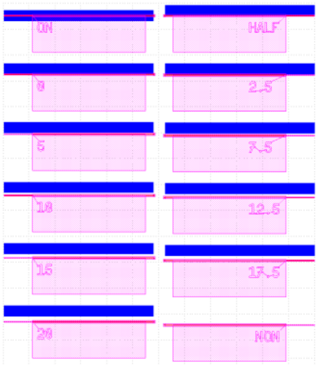

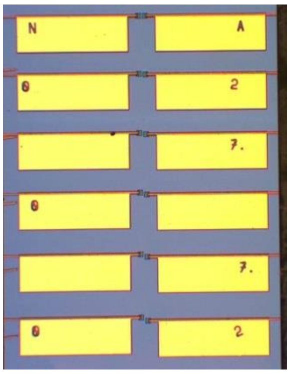

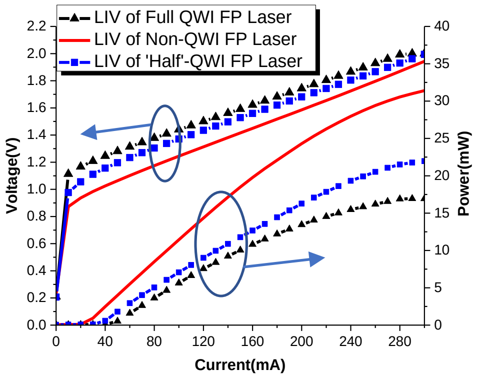

Figure 4. 12 lasers with different distances (the numbers on the chip design represent the distance from edge of the mask to the edge of the ridge) on the QWI boundary (left) and Figure 5. Microscopic picture of the fabricated FP lasers array (middle). Figure 6. Characteristics of current--voltage and output power--current at 20˚C of non-QWI FP laser, 'Half'-QWI FP laser and Full-QWI FP laser (right).

SiN_x mask). The peak lasing wavelength of the non-QWI laser is 1538nm due to the SiO_2 mask protection during the QWI, while the peak wavelength of the full-QWI laser blue-shifts to 1424nm, which proves the success of the QWI process. However, the FP lasers with the ridge waveguide non-fully covered or several microns (0 to around 7.5µm) away from the edge of the SiN_x mask also show a blue-shift of the lasing peak wavelength, but shows less blue shift as the distance increases. When the distance is more than 7.5µm, the QWI effect is no longer observed to affect the lasing performance. This can be clearly seen from Fig.8, which plots the peak lasing wavelengths of the FP lasers annealed at 700˚C and 725˚C with the different distance between the ridge waveguide centre and the edge of the QWI mask.

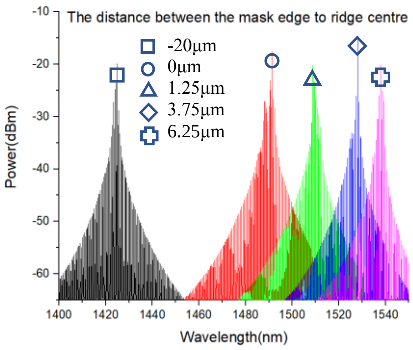

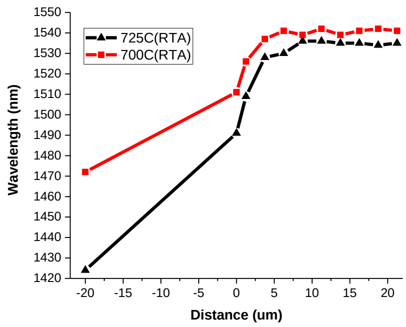

Figure 7. The lasing spectra of the FP laser annealed at 725˚C with different distance between the ridge centre to the edge of the QWI mask (left). Figure 8. The lasing peak wavelength vs the distance between the ridge centre to the edge of the QWI area mask (all the FP lasers are tested under 40mA and the same other condition). Here, "-20" and "0" represent the ridge is in the centre of the mask and half covered by the mask (right).

4. CONCLUSIONS

We have successfully demonstrated a QWI technique using IFVD method with SiN_x by PECVD as promoter and SiO_2 by PECVD as inhibitor and protector. A 120nm blue shift was obtained using InP-based AlInGaAs/AlInGaAs multiple quantum wells, further proved by Fabry-Perot ridge waveguide lasers fabricated with this technique. The QWI mask boundary effect was investigated, which shows the QWI mask edge needs to be more than 7.5µm away from the area where the intermixing is not desired. This QWI technique and the mask boundary effect result will be beneficial for the monolithic integration of photonic devices using AlInGaAs quantum well material.

ACKNOWLEDGEMENTS

This work was supported by the Science Foundation Ireland under Grant SFI 12/RC/2276 and Grant SFI 13/IA/1960.

REFERENCES

[1] M. Smit, K. Williams, and J.V.D. Tol: Past, present, and future of InP-based photonic integration, *APL Photon.* 4, 050901, 2019.

[2] L.P. Hou and J. H. Marsh.: Photonic Integrated Circuits Based on Quantum well Intermixing Techniques. *Procedia Engineering*, vol. 140, pp.107-114, 2016.

[3] J.H. Marsh, P. Cusumano, A.C. Bryce, B.S. Ooi, and S.G. Ayling: GaAs/AlGaAs photonic integrated circuits fabricated using impurity-free vacancy disordering, *Proc. SPIE*, vol. 2401, pp. 74-85, 1995.